Published in final edited form as:
Inorganica Chim Acta. 2010 October 15; 363(12): 2857–2864. doi:10.1016/j.ica.2010.04.004.

Synthesis, characterization, spectroscopy, electronic and redox properties of a new nickel dithiolene system

Partha Basu[1,*], **Archana Nigam**[1], **Benjamin Mogesa**[1], **Suzanne Denti**[1], and **Victor Nemykin**[2]

[1] Department of Chemistry and Biochemistry, Duquesne University, Pittsburgh, PA 15282

[2] Department of Chemistry and Biochemistry, University of Minnesota-Duluth, Duluth, MN 55812

Abstract

A new dithiolene ligand with 3,5-dibromo substituted phenyl groups was designed and synthesized. The protected form of the ligand was reacted with a nickel salt providing neutral $Ni(S_2C_2(3,5\text{-}C_6H_3Br_2)_2)_2$ and anionic $[Ni(S_2C_2(3,5\text{-}C_6H_3Br_2)_2)_2]^-$ isolated as a Bu_4N^+ salt. Both were characterized by UV-visible and IR spectroscopy and compared with the similar known molecular systems. They exhibit intense low-energy transitions that are characteristic of such systems. The electrochemical behavior of these molecules was investigated by cyclic voltammetry.

Introduction

The long standing interest in the development of sulfur coordinated nickel centers stems from their relevance in the biological systems as model complexes for the active sites of nickel enzymes as well as their application in material chemistry. Nickel complexes with sulfur donors are known to exhibit interesting properties such as metallic-conductivity,[1] optical nonlinearity,[2] ability to reversibly react with olefins through a redox couple leading to olefin purification,[3] and strong absorbance in the near infrared region suitable in laser Q-switch dyes.[4] Among these, bis-dithiolene complexes of nickel display important and unusual properties such as very intense electronic transition in the near IR region, capability to exist in different well-defined oxidation states that can be achieved reversibly, and electrical conductivity.[5] These square planar complexes exhibit a high degree of electron delocalization within the chelate ring involving the metal ion that significantly contributes to the low-energy electronic transition between the HOMO and the LUMO, which occurs at an unusually low energy. This extensive electron delocalization, while making these complexes useful as near-infrared (NIR) dyes, is irrelevant to intramolecular charge transfer, a crucial factor in generating second order non-linear optical properties. The delocalized system can exist in three distinct oxidation states: dianionic, monoanionic, and neutral that differ in their spectroscopic signature and magnetic properties. Significant early research has been conducted with unsubstituted or unbranched dithiolene system such as the maleonitrile (Figure 1: **3b** and **3c**). Phenyl substituted dithiolene ligands and their nickel complex was originally synthesized by Schrauzer,[6] which provides an entry towards substituted dithiolene system which can be tailored towards specific function with judicious choice of

basu@duq.edu.

substituents.[7] A majority of the cases though the functionalization is done at the para position of the phenyl group attached to the dithiolene ligand. Herein we report the synthesis, characterization, redox and spectroscopic properties of a new dithiolene nickel system with 3,5-dibromo substituted phenyl groups. These bromo substitution set targets for further development of functionalized materials. These results are complemented with computational analyses using density functional theory. We also report the molecular structure of **3b**.

Experimental

Unless specified all experiments were performed using oven-dried glassware under inert atmosphere using Schlenk (argon) and dry box (nitrogen) techniques. Reagents used in this investigation were of analytical grade and they were purchased either from Aldrich or from Acros Chemical Company and used as received without further purification. Commercial grade solvents were dried and distilled before use: dioxane, hexane, and diethyl ether were dried and distilled over Na-benzophenone; methanol and ethanol were distilled over Mg-turnings; methylene chloride (CH_2Cl_2) was dried and distilled over CaH_2; CH_3CN was distilled over P_2O_5. Anhydrous N,N-dimethylformamide (DMF) was obtained from Acros chemicals. 3,5-dibromobenzaldehyde,[8] **2a**,[6] **2b, 3b** and **3c**,[9] (Figure 1) were synthesized following reported procedures.

Room temperature ^1H and ^{13}C NMR spectra were recorded using a Bruker ACP-300 spectrometer at 300.133 MHz and 75.469 MHz frequencies, respectively. Mass spectra were recorded in a Waters LCQ ESI/APCI Quadrupole Mass spectrometer in ESI and/or APCI modes. Electronic spectra were recorded in Cary 3 or Cary 14 spectrophotometers. Infrared spectra were recorded on a Perkin-Elmer FT-IR 1760X spectrometer on NaCl plates or in KBr pellets. Electrochemical investigations were performed at room temperature using CV-50W voltammetric analyzer with a typical three-electrode system: platinum or graphite-working electrode, Ag/Ag^+ -reference electrode, and Pt wire-auxiliary electrode. 0.1M Tetra butyl ammonium perchlorate (TBAP) was used as a supporting electrolyte. Redox potentials were referenced internally with ferrocenium/ferrocene (Fc^+/Fc) couple. Magnetic susceptibility was measured on a Johnson-Matthey Evans balance, and conductivity was recorded on a VWR conductivity meter. Elemental analyses were performed at Midwest Microlab, LLC, Indianapolis, IN.

Syntheses of 3,3′,5,5′-tetrabromobenzoin and 3,3′,5,5′-tetrabromobenzil

First Method—3,5-dibromobenzaldehyde (300 mg, 1.14 mmol) was dissolved in ethanol (7 mL), which was mixed with an aqueous solution (4 mL) of KCN (36 mg, 0.57 mmol) and stirred for 10 min. The solution was heated overnight at 80 °C in a water bath, and the resulting solution was treated with aqueous $NaHCO_3$ and extracted with chloroform followed by diethyl ether. Both organic layers were washed with saturated aqueous $NaHSO_3$ solution and dried over anhydrous Na_2SO_4. Evaporation of the chloroform layer yielded a pale yellow solid (3,3′,5,5′-tetrabromobenzil, 110 mg, 0.21 mmol) and the ether layer yielded a yellow solid (3,3′,5,5′-tetrabromobenzoin, 50 mg, 0.094 mmol). 3,3′,5,5′-tetrabromobenzil: ^1H NMR ($CDCl_3$): δ= 8.05 (s, 2H, aromatic), 7.8 (s, 1H, aromatic); ^{13}C NMR ($CDCl_3$): δ= 164 (C=O), 138, 134, 131, 123 (aromatic); IR (KBr): 1642 (C=O); yield = 38%. 3,3′,5,5′-tetrabromobenzoin: ^1H NMR ($CDCl_3$): δ = 8.0 (s, aromatic), 7.8 (s, aromatic); 7.5 (s, aromatic), 6.4 (br, s, CHOH), 5.9 (br, s, CHOH); ^{13}C NMR ($CDCl_3$): δ= 164 (C=O), 142, 138, 134, 133, 131, 128, 122 (aromatic), 72 (CHOH); IR (KBr): 1727 (C=O). Yield: 17%.

Second Method—3,5-dibromobenzaldehyde (3.14 g, 11.89 mmol) was dissolved in 12 mL DMF in a Schlenk flask at room temperature. Tetra butyl ammonium bromide (0.32 g,

1.0 mmol) and KCN (0.015 g, 0.211 mmol) were added into the reaction mixture sequentially and the resulting solution was stirred at room temperature for 18–20 h. The solvent was removed by distillation and the resulting residue was poured into water (100 mL) and extracted with CH_2Cl_2. The organic extracts were washed with saturated NaCl solution and dried over anhydrous $MgSO_4$. The gummy material obtained after evaporation of the solvent was crystallized at a low temperature by keeping the material in a refrigerator. The product was recrystallized using CH_2Cl_2/ethanol to obtain pure benzoin as a yellow solid. Yield: 30%, 1.87g (3.56 mmol).

Synthesis of $Ni(S_2C_2(3,5\text{-}C_6H_3Br_2)_2)_2$ (1a)

A mixture of 3,3′,5,5′-tetrabromobenzil or tetrabromobenzoin 0.32 g (0.61 mmol), 2 equivalents of P_4S_{10} (0.53 g, 1.19 mmol) and dry dioxane (7 mL) was placed in a 250 ml Schlenk flask. The reaction mixture was heated at 110 °C for 5–6 h, cooled, filtered to remove unreacted P_4S_{10} and washed with minimum dioxane. To the filtrate, an alcoholic solution (5 mL) of $NiCl_2{\cdot}6H_2O$ (0.16g, 0.68 mmol) was added whereby the color changed to reddish brown. The solution was refluxed with stirring at 90 °C for 2 h, and the reaction flask was capped and kept in refrigerator for 20 h. Excess P_4S_{10} precipitated out and was centrifuged and a clear reddish brown solution was evaporated. The residue was dissolved in a minimal quantity of CH_2Cl_2, and the target compound was precipitated as a green crystalline material by adding methanol. Yield: 12%, 0.082 g (0.07 mmol). Absorption spectrum: (CH_2Cl_2) λ_{max}, nm (ε, $M^{-1}cm^{-1}$): 270 (43000), 316 (60000), 383 (sh, 11800) 582 (2200), 834 (30660); ESIMS (−): 1173 (100%), calculated for $C_{28}H_{12}S_4Br_8Ni$ (M), 1173.

Synthesis of $(Bu_4N)[Ni(S_2C_2(3,5\text{-}C_6H_3Br_2)_2)_2]$ (1b)

The reaction was carried out similar to that for the synthesis of **1a**. A mixture of 3,3′,5,5′-tetrabromobenzil or tetrabromobenzoin (0.94 g, 1.79 mmol), 2 equivalents of P_4S_{10} (1.58 g) and dry dioxane (7 mL) was placed in a 250 ml Schlenk flask. The reaction mixture was heated at 101 °C for 5–6 h, cooled and filtered to remove unreacted P_4S_{10} and washed with minimum dioxane. To the filtrate, an aqueous solution (1 mL) of $NiCl_2{\cdot}6H_2O$ (0.47 g, 1.99 mmol) was added. The mixture was refluxed at 90°C for 2 h and allowed to cool down to room temperature. Tetrabutylammonium bromide was added to the reaction mixture and stirred overnight. The solvent was evaporated, and the oily residue was washed with petroleum-ether several times. The residue was recrystallized from warm CH_2Cl_2 and isopropanol by overnight standing yielding dark reddish violet crystals, which were collected by filtration. Yield: (48%, 0.6 g). Absorption spectrum (CH_2Cl_2) λmax, nm (ε, $M^{-1}cm^{-1}$): 280 (23000), 320 (25000), 380 (sh, 13000), 518 (2000), 680 (500), 934 (5000). ESIMS(−): 1173 (100%) calculated for $C_{28}H_{12}S_4Br_8Ni$ ($[M\text{-}Bu_4N]^-$), 1173.

Synthesis of $Ni(S_2C_2(C_6H_5)_2)_2$ (2a)

In a 500 mL Schlenk flask, benzil or benzoin (5g, 23.8 mmol), P_4S_{10} (21.1g, 47.6 mmol) and dry dioxane (7mL) were added under argon atmosphere and the mixture was refluxed at 110°C for 5–6h. After refluxing, the reaction was filtered to remove unreacted P_4S_{10} and washed with minimal quantity of dioxane. To the filtrate, $NiCl_2{\cdot}6H_2O$ (6.27g, 26.4 mmol) in distilled water (1mL) was added. The mixture was refluxed at 90°C for 2h. A green colored compound was isolated, which was filtered and washed with methanol, water. The crude product was recrystallized using CH_2Cl_2/MeOH. Yield: (30%, 7.19 mmol). Absorption spectrum (CH_2Cl_2) λ_{max}, nm ($\varepsilon_{M,}$ $mol^{-1}cm^{-1}$): 312 (44074), 371 (sh, 10785), 437 (sh, 2643), 596 (1920), 852 (27475). ESIMS(−): 542 (100%) calculated for $C_{28}H_{20}S_4Ni$ (M^-), 542. Anal calcd. C, 61.89; H 3.71. Anal exptl. C, 61.52; H 3.81.

Synthesis of $[Et_4N][Ni(S_2C_2(C_6H_5)_2)_2]$ (2b)

First Method—0.1g, 0.18 mmol of **2a** was dissolved in THF. An acetonitrile solution of Et_4NBH_4 (0.03g, 0.18 mmol) prepared was gradually added to the solution Ni-complex. The color of mixture changed from bluish green to reddish violet. The mixture was stirred for 21 h. The solvent was evaporated to dryness and the residue was redissolved in CH_3CN and filtered to get reddish violet filtrate and orange colored compound as a residue. The filtrate was concentrated and layered with ether to get reddish violet compound, which was dissolved in THF and filtered to get clear reddish violet solution. The solvent was evaporated to give a reddish violet compound. The crude product was further recrystallized from hot acetone and methanol. The reddish purple colored compound was obtained which was washed with methanol and dried in vacuum. Yield: 12% (0.02 mmol). Absorption Spectrum (CH_2Cl_2) λ_{max}, nm ($\varepsilon_{M,}$ $mol^{-1}cm^{-1}$): 264 (38320), 313 (43640), 367 (sh, 12640), 528 (1624), 680 (500), 935 (15217). ESIMS (−): 542 (100%) calculated for $C_{28}H_{20}S_4Ni$ ($[M\text{-}Et_4N]^-$), 542. Anal calcd. C, 64.18; H 5.98; N, 2.08. Anal exptl. C, 64.23; H 6.00; N, 2.18.

Second Method—Complex **2a** (0.500g, 0.92 mmol) and *p*-phenylene diamine (0.25g, 2.3 mmol) were dissolved in dry methyl sulfoxide (10mL). The reaction mixture was stirred and color of mixture changed from dark green to reddish brown. After 2 h of stirring, the mixture was poured into a solution of Et_4NBr (0.42g, 2.01 mmol) in EtOH (15mL). Red crystalline compound was recrystallized using hot acetone/MeOH to give dark purple red compound, which was washed with cold methanol and dried under reduced pressure. Yield: 55% (0.51 mmol).

Reduction of $Ni(S_2C_2(C_6H_5)_2)_2$ (2a)

In a Schlenk flask, fresh sodium (0.01g, 0.37 mmol) was added to a solution of anthracene (0.065g, 0.37 mmol) in 2 mL of THF in anaerobic condition. The dark blue solution was stirred for 6–7 h and then filtered. The filtrate was added drop-wise by a cannula to a solution of **2a** (0.1g, 0.18 mmol) in THF (2mL). The reaction mixture became reddish violet. The solution was stirred overnight and then a solution of Et_4NBr (0.08g, 0.37 mmol) in CH_3CN was added. The solvent was evaporated and the residue was washed with diethyl ether. The residue was dissolved in minimal quantity of acetonitrile, filtered and layered with ether. The dark purple colored compound **2b** was isolated (yield was not measured).

Synthesis of $[Bu_4N]_2[Ni(S_2C_2(CN)_2)_2]$ (3c)

1.71g, 9.24 mmol Na_2mnt ($Na_2S_2C_2(CN)_2$) was dissolved in 30 mL of ethanol/water (1:1) and stirred. This solution was added slowly to another flask containing a solution of $NiCl_2{\cdot}6H_2O$ (1g, 4.2 mmol) in 7.5 mL of H_2O with stirring. A dark red solution was formed, and the stirring continued for another 5 minutes after the addition was complete followed by filtration. To the filtrate, an ethanolic solution of t-Bu_4NBr was slowly added to the filtrate, which separated orange red crystals immediately. The crystals were separated by filtration, washed with H_2O (10 mL) followed by ethanol/water (10 mL, 1:1) and dried. The crude product was recrystallized from hot acetone (80 mL) and isobutyl alcohol (35 mL) for overnight, the crystals were washed with isobutyl alcohol and hexane. Yield: (45.2%, 1.89 mmol.). Absorption Spectrum (CH_3CN) λ_{max}, nm ($\varepsilon_{M,}$ $mol^{-1}cm^{-1}$): 377 (8258), 468 (4474), 514 (1736), 855 (80).

The corresponding dianionic Et_4N^+ salt was synthesized similarly using Et_4NBr as a source of the cation instead of Bu_4NBr. From this dianionic compound, X-ray quality single crystal of the monoanionic complex was prepared in air by slow evaporation of a CH_3CN solution.

Synthesis of $[Bu_4N][Ni(S_2C_2(CN)_2)_2]$ (3b)

An iodine solution (0.3g, 1.2 mmol) in methyl sulfoxide (1 mL) was added to the solution of dianionic complex of $[Bu_4N]_2[Ni(S_2C_2(CN)_2]$ (0.5g, 0.75 mmol) in methyl sulfoxide (4 mL). The mixture was immediately added to ethanol (12.7mL) and stirred for 20–30 min at room temperature. The black crystalline compound was isolated, filtered and washed with ethanol (5–6 times) followed by ether. The compound was recrystallized by dissolving the compound in hot acetone and adding ether. Keeping the mixture overnight at room temperature gives black crystalline compound. Yield: (65.3%, 0.4 mmol). Absorption spectrum (CH_3CN) λ_{max}, nm ($\varepsilon_{M,}$ $mol^{-1}cm^{-1}$): 346 (sh, 11372), 475 (2510), 538 (670), 602 (461), 863 (9700). mass spectra (m/z) (ESI-): 338 (100%, m/z) [$C_8S_4N_4Ni$ ([M-Bu_4N]$^-$), 338].

X-ray Crystallography

X-ray quality single crystals were selected under the microscope, and mounted on glass fibers. X-ray intensities were measured on a Rigaku AFC-7R four-circle diffractometer using graphite-monochromatized Mo *Kα* radiation (λ = 0.71069Å) at room temperature using the ω−2θ scan technique. Three standard reflections were measured every 150 reflections; a linear correction factor was applied. The structure of complex was initially solved by Patterson method using TeXsan crystallographic software package of Molecular Structure Corporation[10] then they were refined using Crystals for Windows package.[11] The cut off limit for the reflection was $I>2\sigma(I)$. Selected crystal data for **3b** are presented in Table 1.

Computational Methods

All calculations were carried out using Gaussian 03W software package.[12] For the electronic structure calculations, all geometries were optimized at DFT level of theory using BP86 exchange correlation functional and 6–311G(d) basis set for all atoms. Frequency calculations were conducted on all optimized structures in order to ensure the optimized structures represent a local minimum. The percentages of atomic orbital contributions to their respective molecular orbitals were calculated by using the VMOdes program. [13]

Results and Discussion

Syntheses and Characterization

The synthetic strategy for 3,5-dibromophenyl dithiolene ligand and its nickel complexes $[Ni\{C_2S_2(3,5\text{-}C_6H_3Br_2)_2\}_2]^{0,-1}$ (**1a** and **1b**) is presented in Scheme 1. The starting material 3,5-dibromobenzaldehyde was synthesized from commercially available 1,3,5-tribromobenzene following a reported method in good yield.[8] 3,3′,5,5′-tetrabromo benzoin as well as 3,3′,5,5′-tetrabromo benzyl were synthesized from 3,5-dibromobenzaldehyde following benzoin condensation reaction, which were purified by extraction with diethyl ether and chloroform respectively, and were characterized by ^1H, ^{13}C NMR and IR spectroscopy. The ^1H NMR spectrum for benzil revealed a symmetric structure, while that of benzoin exhibits two CHOH resonances at 6.4 and 5.9 ppm. The yields for both benzil and benzoin were moderate (17% for benzoin and 38% for benzil) due to the deactivating nature of the Br-group at the *meta* positions of the phenyl ring. However, better yield for 3,3′,5,5′-tetrabromobenzoin (30%) was achieved when 3,5-dibromobenzaldehyde was reacted directly with KCN and Bu_4NBr in DMF.[14]

As benzil and benzoin are reported to form the same thiophosphoric ester,[15] both 3,3′,5,5′-tetrabromobenzoin and 3,3′,5,5′-tetrabromobenzil were reacted with P_4S_{10} under inert atmosphere forming the thiophosphoric ester, which was used in preparing the nickel complex.

Complex **1a** and the alkyl ammonium salt, **1b** were obtained following the method initially developed by Schrauzer *et al* [6] and later modified by Holm *et al*. [15] The mechanistic details of this reaction has recently been elucidated by Arumugam et al through isolation and structural characterization thiophosphoryl compound.[16] Reaction of thiophosphoric ester with Ni(II) salts, hydrated $NiCl_2$, gave a reddish-brown solution (Scheme 1). The green colored neutral **1a** was isolated from CH_2Cl_2 at a low temperature (5 °C). Complex **1b** was synthesized by using an analogous procedure for **1a** i.e., direct reaction between the metal and the pro-ligand. Here thiophosphoric ester was refluxed with $NiCl_2$ followed by precipitation of the tetrabutylammonium salt using Bu_4NBr as a precipitant. The compound was initially obtained as a reddish violet oil, which was washed with petroleum ether and recrystallized from CH_2Cl_2 to get a reddish violet needle shaped crystalline compound. A neutral nickel complex, $Ni(C_2S_2Me_2)_2$, has been successfully reduced to dianionic $[Ni(C_2S_2Me_2)_2]^{2-}$ using sodium anthracide.[17] Similar attempts to synthesize dianionic $[Ni\{C_2S_2(3,5\text{-}C_6H_3Br_2)_2\}_2]^{2-}$ were unsuccessful, although neutral **2a** could be reduced to monoanaionic **2b**. Similarly, synthesis of neutral maleonitrile complex (i.e., neutral **3a**) through oxidation of **3b**, or **3c** was also not successful. Thus, poising of redox potentials play a major role in stabilizing a specific oxidation state, and the redox potentials can be modulated by suitable substituents (*vide infra*).[18]

The compositions of the complexes were confirmed by electrospray ionization mass spectrometry (ESIMS) in the negative ion mode. The characteristic molecular ion peaks for complexes were detected with ~100% intensity. Both **1a** and **1b** gave peak clusters with a base peak with mass to charge ratio at 1173 consistent for $[M]^-$ for **1a** and $[M\text{-}Bu_4N]^-$ for **1b** respectively. Conductivity of complexes was measured in nitromethane solutions at room temperature (Table 2). **1b** exhibits characteristic conductivity for a 1:1 complex like **3b**,[19] while **1a** was non-conducting indicating its electroneutrality. Solid state magnetic susceptibilities of **1b** at 293 K showed paramagnetism with spin only value corresponds to one unpaired electron (Table 2), whereas **1a** is diamagnetic. These measurements probed the neutral and mono-anionic nature of **1a** and **1b** respectively, indicating that metal ion is formally in +3 oxidation state in **1b**, dithiolene acts as a monoanionic ligand i.e., in its oxidized form. ESIMS of **3b** gave a molecular ion at ~338 peak due to anionic $[Ni(S_2C_2(CN)_2)_2]^-$ whose isotope distribution pattern matches well with that of the calculated molecular ion. The corresponding dianionic complex (**3c**) a peak cluster was observed at the same m/z value even though the electronic spectra of the solution is different and showed a 2:1 electrolyte. This suggests that during the mass spectral analyses the complex is oxidized. Such oxidation chemistry under mass spectrometric conditions has been observed before in transition metal chemistry.[20]

Electronic Spectroscopy—The electronic spectroscopy is an excellent tool to define the neutral or anionic nature of the Ni-dithiolene complexes. A strong absorption band at the low energy region (near IR region) is a characteristic of neutral complex, which shifts to a lower energy with less intensity in the monoanionic complex and this band is not present in the dianionic complex. Electronic spectra of **1a** and **1b** were recorded in CH_2Cl_2 (Figure 2). Compounds **3b** and **3c** were insoluble in CH_2Cl_2 and spectra were recorded in CH_3CN. Figure 2 also shows electronic spectra **2a**, **2b**, **3b**, and **3c**.

High level density functional calculations[21] on $Ni(S_2C_2Me_2)_2$ suggest the ground state to be $\ldots(18a_{1g})^2(4b_{3g})^2(6b_{1u})^2(5b_{2g})^0(13b_{1g})^0\ldots$In the neutral species, the HOMO is the b_{1u} orbital is fully occupied which is primarily ligand based with minor contribution from the metal. The intense charge transfer absorption is due to the transition from $b_{1u} \rightarrow b_{2g}$ transition. The b_{2g} orbital in the one-electron reduced monoanionic species is singly occupied. The contributions from nickel to this b_{2g} orbital increase with reduction, and the band position also shifts. Because of the involvement of the dithiolene orbitals, the position

of the low energy transition is dependent on the substituent on the dithiolene ligand itself. For example, in monoanionic complexes the low energy band shifts to lower energy with increasing electron-releasing character of the substituent. The results presented in here indicate that the effect of distal substituents (ca. the substituents on the phenyl ring that is attached to the dithiolene) is small. The electronic spectra show some variation: the first band near 852 nm for the **2a** shifts to 834 nm, a shift of 18 nm, while 935 nm band in **2b** moved to 927 nm in **1b**, which is only an 8 nm shift. However, this band shifts to 863 nm in the case of **3b**. With the exception of **3c** no other dianionic species was isolated where this band is absent. Thus, the low energy band maxima follow the order: **1b** ~ **2b** > **3b**. This is consistent with the reported results on neutral complexes of general formula, $Ni\{(S_2C_2(p\text{-}C_6H_4X)_2\}_2$.[15] The intensities of these band in three compounds are different, **3b** being the least intense. Because the intensity comes from the mixing of the orbital coefficients involved in the optical transition, it is suggestive that the ground and the excited states do not mix as efficiently, and inclusion of the phenyl ring increases the mixing perhaps by lowering the symmetry. Thus, while significant differences exist going from localized dithiolene to phenyl substituted dithiolene, there little difference with substitution on the phenyl ring.

Electrochemical Properties—Electrochemical properties of all complexes were investigated by cyclic voltammetry in CH_2Cl_2 (compounds **1a** and **1b**) or CH_3CN (**3b** and **3c**). Cyclic voltammogram of **1a** is shown in Figure 3. Two quasi-reversible one-electron redox couples were observed for **1a** and **2a**, while only one redox couple was observed for **3b.** A detailed spectroscopic study on **3b** (monoanionic) suggests that the singly occupied molecular orbital (SOMO) of this compound largely dominated by sulfur from the dithiolene ligand, which underscores the highly delocalized nature of the metal-sulfur orbitals in these molecules.[21] Our electronic structure calculations, detailed later, are in good agreement with the precious findings. Thus, assigning the redox potentials only to metal based orbitals is ambiguous at best. We therefore designate the redox potentials in terms of the overall charge of the molecule – neutral (N), monoanionic (M) to dianionic (D), and these species are related by equation 1.

$$N \underset{-e}{\overset{+e}{\rightleftharpoons}} M \underset{-e}{\overset{+e}{\rightleftharpoons}} D \qquad \text{(Equation 1)}$$

It is interesting to note that maleonitrile complexes (**3**) exhibited only one redox couple at −260 mV, which is due to the M/D couple. This couple is moved significantly cathodically in the phenyl substituted compounds by 800 mV and 1013 mV for molecular systems **1** and **2**, respectively. Thus, introduction of the highly electron withdrawing nitrile group moves the N/M couple beyond the solvent window. Interestingly this couple has been proposed to lie beyond 1 V,[17] which is consistent with the difficulty in the synthetic procedures described here.

Compared to the unsubstituted phenyl derivative, introduction of electron withdrawing Br-groups also influences the redox potentials. The direction of the change in the M/D couple is however, in the expected order. Introduction of eight Br-groups in the molecule shifts the redox potential towards more positive direction. Interestingly, the difference between the two couples N/M-M/D is smaller in the case of Br-substituted compound. Thus, clearly redox orbital (b_{1u}) in this case is influenced significantly by the substitution at the phenyl ring. However, the direction of shift for the N/M couple is counter intuitive, which becomes more difficult by 30 mV for **1** compared to **2**. Taking together, the redox properties of these

complexes are influenced by the substituents on the dithiolene ligands because of the ligand-based nature of the HOMO.

Molecular Structure

X-ray quality single crystals of $[Et_4N][Ni(S_2C_2(CN)_2)_2]$ were obtained by slow evaporation of an CH_3CN solution of $[Et_4N]_2[Ni(S_2C_2(CN)_2)_2]$ in air. It is interesting to point out that the structure of this compound has been solved before with different cell parameters and space groups.[22] The structure of this complex was as expected with very little unusual features and thus the discussion will be limited. The Ni-S distances are as expected 2.14 Å, and the bite angles of the two ligands are ~92°. The molecular structure is shown in Figure 4. The nickel center shows a square planar geometry coordinated by the four sulfur donors of the two dithiolene ligands. We were pleased with no disorder problem with the ethyl groups of the cation, which often exhibit a positional disorder. The packing diagram of the complex (Figure 5) shows that the planar Ni-complexes are stacked and in between the layers, the tetraethyl ammonium ions are positioned, which may explain rigidity of the tetraethyl ammonium groups.

Electronic Structure

The electronic structures of the Ni-complexes were investigated by density functional theory using optimized geometries. The $[Ni(S_2C_2(CN)_2)_2]^{-1/-2}$ exhibited a D_{2h} symmetry while that for the phenyl complexes was converged to D_2 point group. The monoanionic complexes were calculated using spin-unrestricted model, while neutral and dianionic complexes were calculated with a spin restricted model.

The compositions of the frontier orbitals are listed in Table 3 and energy levels are shown in Figures 6 and 7, and pictorial representations of selected orbitals are presented in Figure 8. The compositions the HOMO and the LUMO of **1b**, **2b** and **3b** show small difference. In all cases metal and the sulfur orbitals contribute significantly, however, incorporation of phenyl rings in the ligand architecture reduces the metal electron density by ~10%. There is virtually no difference in the orbital compositions with and without the Br-substitution in the phenyl ring. The high S contributions in the frontier orbitals indicate a facile electron delocalization pathway involving the Ni and sulfur orbitals underscoring the importance of the non-innocent nature of the dithiolene ligand. The presence of the phenyl ring impacts the energetic more significantly; the HOMO in **3b** is stabilized by 1.5 eV due to the electron donating phenyl group. The destabilization caused by phenyl ring is attenuated (by ~0.8 eV) in **1b** due to the presence of the electron withdrawing Br-derivative. Interestingly, the HOMO-LUMO separation is not significantly different, the maximum difference being 0.2 eV. This indicates that introduction of the phenyl ring while does not significantly alter the orbital composition, but the overall energies are affected, which of course can influence not only the reduction potentials but also the optical spectra. A similar situation has been observed in X-ray absorption spectroscopy.[21,23]

The diamagnetic compounds are different such that compound **1a** and **2a** are neutral, compound **3c** is dianionic. The frontier orbitals in **1a** and **2a** are much more stabilized than those in **3c**, although the HOMO-LUMO gap differs only by 0.1 eV. The orbitals compositions are significantly different: metal contribution to HOMO in **1a** and **2a** is virtually negligible, but that in **3c** substantial. Contribution from the S orbitals to the HOMO is 35% in **1a** and **2a** which is ~10% than that in **3c**. In **3c** both Ni and S contributes equally to the HOMO. These differences not only affect the physical properties but also impact their chemical reactivity.

Summary

We have designed and synthesized new nickel dithiolene complexes containing 3,5-$C_6H_3Br_2$ substituted phenyl groups. Compounds (**1a** and **1b**) have been characterized by NMR, UV-visible, and IR spectroscopy. The redox potentials exhibit exquisite sensitivity with respect to the substituents and the optical spectra show little variation (in similarly charged molecular systems like **1a** and **2a**). The differential sensitivity is a result of different alignment of the redox orbitals. We determined the molecular structure of the **3b**, and the electronic structures of **1b**, **2b**, and **3b** show a variation in the energies of the orbitals without significantly effecting the composition. Similar calculations on diamagnetic **1a**, **2a** and **3c** indicate not only a difference in energy but also compositional variation of frontier orbitals.

Supplementary Material

Refer to Web version on PubMed Central for supplementary material.

Acknowledgments

We thank Dr. Raghvendra S. Sengar for insightful discussions. Financial assistance from the National Institutes of Health (GM061555) is gratefully acknowledged. We also acknowledge the Minnesota Supercomputing Institute for the generous support of computer time.

References

1. Tanaka H, Okano Y, Kobayashi H, Suzuki W, Kobayashi A. Science 2001;291:285. [PubMed: 11209074]
2. Oliver SN, Kershaw SV, Underhill AE, Hill CAS, Charlton A. MCLC S&T, Section B: Nonlinear Optics 1995;10:87.
3. Wang K, Stiefel EI. Science 2001;291:106. [PubMed: 11141557]
4. Mueller-Westerhoff UT, Vance B, Yoon DI. Tetrahedron 1991;47:909.
5. a) Baudron SA, Avarvari N, Batail P. Inorg Chem 2005;44:3380. [PubMed: 15877415] b) Cho JY, Domercq B, Jones SC, Yu J, Zhang X, An Z, Bishop M, Barlow S, Marder SR, Kippelen B. J Mater Chem 2007;17:2642. c) Cho JY, Fu J, Padilha LA, Barlow S, Van Stryland EW, Hagan DJ, Bishop M, Marder SR. Mol Cryst Liq Cryst 2008;485:915. d) Hill CAS, Charlton A, Underhill AE, Malik KMA, Hursthouse MB, Karaulov AI, Oliver SN, Kershaw SV. J Chem Soc, Dalton Trans: Inorg Chem 1995:587. e) Jeannin O, Clerac R, Fourmigue M. Chem Mater 2007;19:5946.
6. Schrauzer GN, Mayweg V. J Am Chem Soc 1962:3221.
7. Madhu V, Das SK. Inorg Chem 2008;47:5055. [PubMed: 18479121]
8. Chen LS, Chen GJ, Tamborski C. J Organomet Chem 1981;215:281.
9. a) Davison A, Edelstein N, Holm RH, Maki AH. Inorg Chem 1963;2:1227. b) Davison A, Edelstein N, Holm RH, Maki AH. J Am Chem Soc 1963;85:2029.
10. Molecular Structure Corporation 1985 and 1992.
11. Betteridge PW, Carruthers JR, Cooper RI, Prout K, Watkin DJ. J Appl Crystallogr 2003;36:1487.
12. Frisch, GWTMJ.; Schlegel, HB.; Scuseria, GE.; Robb, MA.; Cheeseman, JR.; Montgomery, JA., Jr; Vreven, T.; Kudin, KN.; Burant, JC.; Millam, JM.; Iyengar, SS.; Tomasi, J.; Barone, V.; Mennucci, B.; Cossi, M.; Scalmani, G.; Rega, N.; Petersson, GA.; Nakatsuji, H.; Hada, M.; Ehara, M.; Toyota, K.; Fukuda, R.; Hasegawa, J.; Ishida, M.; Nakajima, T.; Honda, Y.; Kitao, O.; Nakai, H.; Klene, M.; Li, X.; Knox, JE.; Hratchian, HP.; Cross, JB.; Adamo, C.; Jaramillo, J.; Gomperts, R.; Stratmann, RE.; Yazyev, O.; Austin, AJ.; Cammi, R.; Pomelli, C.; Ochterski, JW.; Ayala, PY.; Morokuma, K.; Voth, GA.; Salvador, P.; Dannenberg, JJ.; Zakrzewski, VG.; Dapprich, S.; Daniels, AD.; Strain, MC.; Farkas, O.; Malick, DK.; Rabuck, AD.; Raghavachari, K.; Foresman, JB.; Ortiz, JV.; Cui, Q.; Baboul, AG.; Clifford, S.; Cioslowski, J.; Stefanov, BB.; Liu, G.; Liashenko, A.; Piskorz, P.; Komaromi, I.; Martin, RL.; Fox, DJ.; Keith, T.; Al-Laham, MA.; Peng,

CY.; Nanayakkara, A.; Challacombe, M.; Gill, PMW.; Johnson, B.; Chen, W.; Wong, MW.; Gonzalez, C.; Pople, JA. Gaussian, Inc. Pittsburgh PA: 2003.

13. Nemykin VN, Basu P. 2003
14. Cameron JF, Willson CG, Frechet JMJ. J Chem Soc, Perkin Trans 1 1997:2429.
15. Sung KM, Holm RH. J Am Chem Soc 2002;124:4312. [PubMed: 11960460]
16. Arumugam K, Bollinger JE, Fink M, Donahue JP. Inorg Chem 2007;46:3283. [PubMed: 17358055]
17. Lim BS, Fomitchev DV, Holm RH. Inorg Chem 2001;40:4257. [PubMed: 11487330]
18. Vogler A, Kunkely H. Angew Chem 1982;94:63.
19. Geary WJ. Coord Chem Rev 1971;7:81.
20. a) Nemykin VN, Basu P. Dalton Trans 2004:1928. [PubMed: 15252579] b) Nemykin VN, Basu P. Inorg Chim Acta 2005;358:2876.
21. Huyett JE, Choudhury SB, Eichhorn DM, Bryngelson PA, Maroney MJ, Hoffman BM. Inorg Chem 1998;37:1361. [PubMed: 11670347]
22. a) Mahadevan C, Seshasayee M, Radha A, Manoharan PT. Acta Crystallogr, Sect C: Cryst Struct Commun 1984;40:2032. b) Kobayashi A, Sasaki Y. Bull Chem Soc Jpn 1977;50:2650. c) Mochida T, Suzuki S, Moriyama H, Terao H, ST. Acta Crystallogr, Sect C: Cryst Struct Commun 2000;56:1183.
23. a) Szilagyi RK, Lim BS, Glaser T, Holm RH, Hedman B, Hodgson KO, Solomon EI. J Am Chem Soc 2003;125:9158. [PubMed: 15369373] b) Sarangi R, DeBeer George S, Rudd DJ, Szilagyi RK, Ribas X, Rovira C, Almeida M, Hodgson KO, Hedman B, Solomon EI. J Am Chem Soc 2007;129:2316. [PubMed: 17269767]

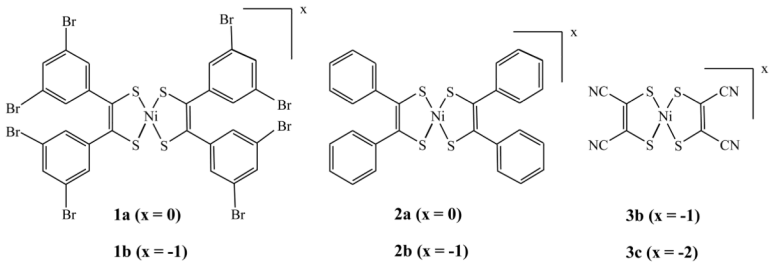

Figure 1.
The compounds used in this investigation.

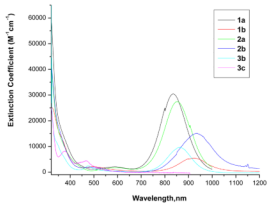

Figure 2.

Electronic spectra of Ni-complexes recorded at room temperature.

1a, **1b**, **2a**, and **2b** were recorded in CH_2Cl_2. **3b** and **3c** were recorded in CH_3CN.

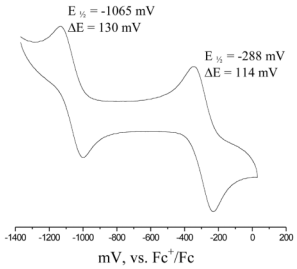

Figure 3.
Room temperature cyclic voltammogram of **1a** in CH_2Cl_2.

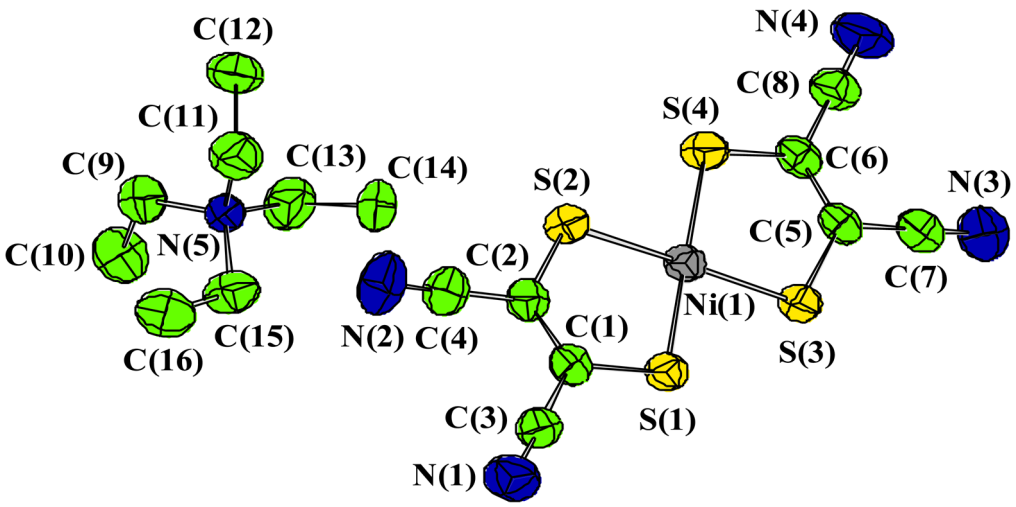

Figure 4.
Thermal ellipsoid (50% probability) representation of molecular structure of $[NEt_4][Ni(S_2C_2(CN)_2)_2]$.

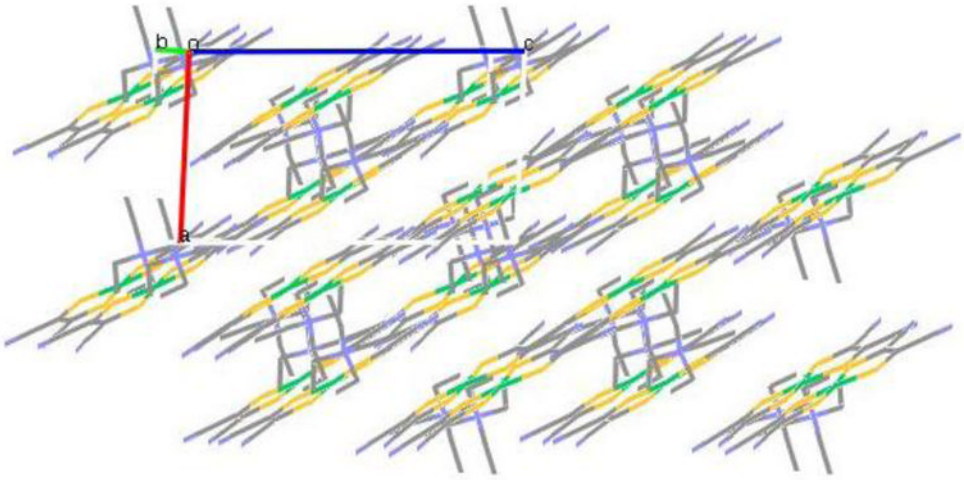

Figure 5.
Packing diagram of $[NEt_4][Ni(S_2C_2(CN)_2)_2]$.

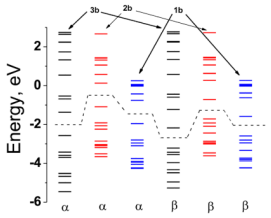

Figure 6.
Molecular orbital diagram of **3b, 2b,** and **1b** calculated in spin unrestricted DFT method. The dashed line represents the separation between the HOMO and the LUMO. The formal oxidation state of Ni in these complexes is considered to be +3.

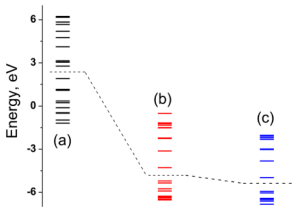

Figure 7.
Molecular orbital diagram of **3c** (a), **2a** (b) and **1a** (c) calculated in spin restricted DFT method. The dashed line represents the separation between the HOMO and the LUMO.

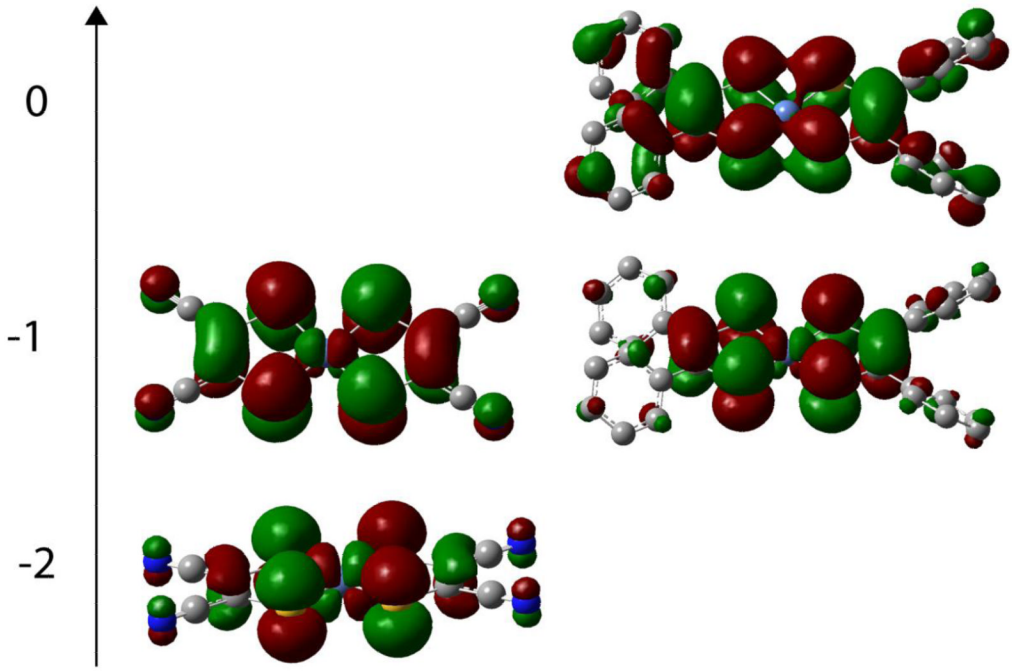

Figure 8.
Pictorial representation of the HOMOs. The complexes are arranged vertically in order of increasing charge. The left panel shows complex **3** while the right panel shows complex **2.**

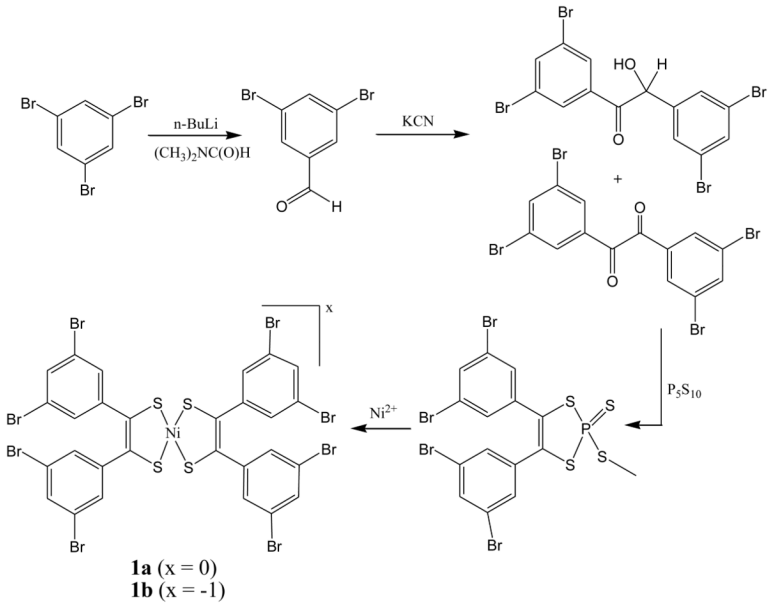

Scheme I.

Table 1

Crystallographic data for **3b**.

	3b
Formula	$C_{16}H_{20}N_5S_4Ni$
Fw	469.34
Crystal system	Monoclinic
Space group	$P2_1/n$
a, Å	8.180(3)
b, Å	18.411(3)
c, Å	14.435(3)
β, deg	92.79(2)
V, Å^3	2171.3(10)
Z	4
ρ_{calcd} (g cm^{-1})	1.44
Data collected	4238
R(F^2)	0.0476
wR(F^2)	0.1176
Max. residual electron density	0.51

Table 2

Characterization data for the nickel complexes used in this investigation.

Complex	Base Peak in ESI-MS	UV-Vis Spectra ε (λ,nm) $M^{-1}cm^{-1}$	$E_{1/2}$ (ΔE) mV vs. Fc^{+}/Fc	μ_{eff}, B.M.	Λ_M Ohm^{-1} cm^2 mol^{-1} in nitromethane
1a	1173	30,660 (834)	−288 (114)	0	Non-conducting
1b	1173	6500 (927)	−1065 (130)	1.77	63
2a	542	27,500 (852)	−258 (94)	0	Non-conducting
2b	542	15,200 (935)	−1275 (133)	1.82	68
3c	338	80 (855)	−262 (68.5)	0	187
3b	338	9700 (863)		1.54	69

Table 3

The composition of selected orbitals.

Compound		Orbital	Symmetry	Energy, eV	% Ni	% S
1b	α	HOMO−1	B3	−2.796	49.6	15.1
		HOMO	B2	−1.951	13.4	49.2
		LUMO	B1	−0.754	16.6	33.1
		LUMO+1	A	−0.426	0.40	12.5
	β	HOMO−1	B1	−2.804	0.70	46.9
		HOMO	B3	−2.587	48.2	13.7
		LUMO	B2	−1.579	21.9	43.2
		LUMO+1	B1	−0.621	16.5	30.4
2b	α	HOMO−1	B3	−1.919	51.5	15.7
		HOMO	B2	−1.088	14.0	51.0
		LUMO	B1	0.130	17.7	36.3
		LUMO+1	A	0.583	0.5	13.3
	β	HOMO−1	B1	−1.921	0.7	45.9
		HOMO	B3	−1.712	50.2	14.3
		LUMO	B2	−0.719	23.0	45.2
		LUMO+1	B1	0.270	17.9	34.2
3b	α	HOMO−1	B1g	−3.426	64.9	17.3
		HOMO	B2g	−2.566	16.5	62.7
		LUMO	B3g	−1.371	18.6	35.9
		LUMO+1	B1g	−0.682	2.7	19.1
	β	HOMO−1	B3u	−3.435	0.7	55.9
		HOMO	B1g	−3.215	64.5	15.7
		LUMO	B2g	−2.178	27.6	56.6
		LUMO+1	B3g	−1.221	19.0	34.2
1a		HOMO−1	B3	−6.042	48.6	17.0
		HOMO	B1	−5.932	0.7	36.9
		LUMO	B2	−4.977	13.5	49.6

Inorganica Chim Acta. Author manuscript; available in PMC 2011 October 15.

Compound	Orbital	Symmetry	Energy, eV	% Ni	% S
	LUMO+1	B1	−3.821	18.3	37.0
2a	HOMO−1	B3	−5.345	50.1	17.6
	HOMO	B1	−5.212	0.8	35.8
	LUMO	B2	−4.283	13.8	50.4
	LUMO+1	B1	−3.125	18.7	38.3
3c	HOMO−1	Ag	1.159	85.1	7.7
	HOMO	B2g	1.916	47.6	43.0
	LUMO	B3g	2.771	20.6	32.9
	LUMO+1	B1g	3.049	5.6	21.3